Journal of Marine Research, 65, 491–522, 2007

Simulated fiddler-crab sediment mixing

by Katherine Huang[1], Bernard P. Boudreau[1,2] and Daniel C. Reed[1]

ABSTRACT

Using a lattice-automaton model, we simulate the effects of fiddler crabs on the distribution of excess ^{210}Pb in marsh sediments. Three previously-identified modes of bioturbation are investigated: (1) *removal-and-fill*, where material is excavated to the sediment-water interface and burrows, when abandoned, are subsequently filled by surface material, (2) *removal-and-collapse*, where the infilling occurs by collapse of the burrow walls, and (3) *partial-compaction-and-collapse*, where part of the excavated sediment is packed into the burrow wall and abandoned burrows subsequently collapse. These various mixing modes lead to somewhat different laterally-integrated $^{210}Pb_{ex}$ profiles, which are also influenced by burrowing frequency, burrow dimensions, fraction of surface material replaced by new sediment (regeneration), and the fraction of material compacted during burial.

Using parameters from a previous study in a South Carolina marsh, we find that data from low-marsh sites are best predicted by the partial-compaction-and-collapse process; this is consistent with the observation that burrow casts indicate far more material is excavated than is deposited as pellets at the sediment-water interface. The profile from the high-marsh site is best simulated by removal-and-fill mixing, with 50% regeneration of material at the sediment-water interface; this is consistent with less frequent flooding at this site.

We have also calculated the exchange function for each of these mixing modes and show that they are highly asymmetric, indicating that the mixing is not diffusive. Only in the case of partial-compaction-and-collapse does the exchange function approach a diffusive form when the excavation rate decreases, i.e., the probability of compaction increases.

1. Introduction

Bioturbation, the mixing of sediment particles by benthic fauna, affects most fine-grained marine sediments. Organisms actively displace sediment grains through everyday processes, such as feeding, burrowing, and construction of living quarters. Furthermore, particles are also transported via passive mechanisms, including particles falling into burrows or tubes and infilling of abandoned structures. Bioturbation is frequently the dominant particle transport process in sedimentary deposits and, consequently, of paramount importance to the distribution of biologically and geochemically relevant species. This provides motivation for developing a quantitative understanding of biogenic mixing processes.

1. Department of Oceanography, Dalhousie University, Halifax, Nova Scotia, B3H 4J1, Canada.
2. Corresponding author. ***email: bernie.boudreau@dal.ca***

Studying bioturbation, however, is not straightforward, as subsurface processes are normally not subject to *direct* visual observation. Instead, particle-bound tracers and introduced particles are the principal tools used to quantify rates of bioturbation, but these come with significant limitations and costs. For example, tracer techniques are often labor-intensive and time-consuming, e.g., counting luminophores. Moreover, the resulting profiles are integrative, representing the total mixing effect by all the various mixing modes at work and, thus, offer little evidence regarding specific mechanisms of sediment transport.

To address these limitations while providing the ability to examine individual mixing mechanisms and various behavioral strategies, we have developed a simulation environment, LABS (Lattice-Automaton Bioturbation Simulator) that reproduces a functioning bioturbated sediment within a computer-environment (Choi *et al.*, 2002). The sediment is simulated as a collection of quasi-particles on a regularly spaced matrix. Within the sediment-water matrix, infauna are represented as automata that are governed by rules set by the programmer and intended to capture the behavior of real benthic organisms. Tracers can be employed in the same way that they are in the field, by tagging particles with radioisotopes or introducing "luminophores". What results is a simulation environment that can be easily manipulated and sampled rapidly, all at little cost. The generated output can be used to supplement our database of field and laboratory observations and to advance our understanding of bioturbation. Filip Meysman (NIOO) has drawn the following analogy: "LABS is to sediments what a flight-simulator is to real aircraft." That is, LABS provides a cost-effective opportunity to examine various scenarios that cannot be studied in nature or the laboratory due to experimental, temporal or financial constraints. Furthermore, as we have absolute knowledge of the system, the very fundamentals of bioturbation can be analyzed, thus providing unprecedented insight.

The synthetic data generated by LABS can be analyzed with standard inverse models, e.g., biodiffusion or nonlocal models, in an attempt to directly link biological actions to common conceptual parameter, e.g., D_B. This has already been proven to be a fruitful means of investigation (Reed *et al.*, 2006). In this paper, we apply LABS to examine fiddler-crab-induced bioturbation and its effect on excess ^{210}Pb profiles.

Fiddler crabs are one of the most abundant macrofauna found in intertidal salt marshes (Katz, 1980; Montague, 1980, 1981). The burrowing activities of fiddler crabs are a major cause of bioturbation in salt marshes, affecting their biogeochemistry by promoting sediment and pore water exchange (Gribsholt *et al.*, 2003; Katz, 1980; Koretsky *et al.*, 2002; Kristensen and Alongi, 2006; Nielsen *et al.*, 2003). These crabs burrow, vertically or sub-vertically, to depths between 10 to 25 cm, excavating sediment to the surface. This excavated sediment can be washed away and replaced by "new" material in areas regularly flushed by tides (Benninger *et al.*, 1979; Sharma *et al.*, 1987), a process termed "regeneration". Abandoned burrows are later filled by this new surficial material (Sharma *et al.*, 1987) and/or by the collapse of the burrow walls (McCraith *et al.*, 2003).

Bioturbation by fiddler crabs is considered to be highly directional, nonlocal mixing,

because the exchange of materials by burrowing and infilling is principally between widely separated points within the sediment column (Boudreau and Imboden, 1987). Consequently, the diffusion analog, which is commonly used to model the effects of bioturbation of particle-bound radionuclides, is likely inappropriate in this case. Gardner *et al.* (1987) first proposed a model to describe the effects of fiddler-crab burrowing. This model assumes that the excavated sediment is washed away and back-filled by an equal volume of sediment with a constant (input) tracer concentration/activity. Therefore, the depth (z) distribution of the steady-state tracer $^{210}Pb_{ex}$, with constant input activity, and assuming constant bulk density and porosity, is governed by the equation

$$\frac{d(^{210}Pb)}{dz} = \frac{-\lambda(^{210}Pb)}{S} - \frac{K_B(^{210}Pb)e^{(-z/U_B)}}{S} + \frac{K_B(^{210}Pb_0)e^{(-z/U_B)}}{S} \quad (1)$$

where S is the sedimentation rate (cm y^{-1}), λ is the decay constant of ^{210}Pb (y^{-1}), $^{210}Pb_0$ is the surface activity of the tracer (dpm), K_B is the burrowing frequency (y^{-1}), and U_B is the mean burrow depth (cm). The first term on the right-hand side of the equation describes the decay of $^{210}Pb_{ex}$, while the second and third terms describe the change of this tracer's activity when the sediment at depth is replaced with surface sediment, assuming that the probability of a burrow reaching or exceeding a depth z is distributed exponentially.

The validity of this (regeneration) model rests on the following assumptions: (1) the excavated sediment is completely replaced by source material with a constant input activity; (2) burrows are completely filled-in with surficial source materials, without any collapse of the burrow walls; (3) burrows are formed by excavation from depth to the sediment surface, without packing any material into the burrow wall and, as stated above, and (4) there is an exponential distribution of burrow lengths. Real fiddler-crab mixing has proven to be much more complicated than this simple model would suggest and, therefore, may not meet these assumptions. For example, some high-marsh sites are not flushed by tides on a regular basis, so that the back-fill sediments are not completely replaced with new source materials. On the other hand, at regularly flooded low and muddy marsh sites, the abandoned burrows may be filled by burrow wall collapse, which was suggested as the reason that the regeneration model could not provide a good fit to observed $^{210}Pb_{ex}$ profiles (McCraith *et al.*, 2003). In this latter case, profiles predicted by the model using direct field measurements of burrowing parameters were higher in activity and were more vertical than observed profiles.

McCraith *et al.* (2003) modified the second term in the previous regeneration model to account for the effects of burrow-wall collapse:

$$\frac{d(^{210}Pb)}{dz} = \frac{-\lambda(^{210}Pb)}{S} - \frac{K_B(^{210}Pb)e^{(-z/U_B)}}{S} + \frac{K_B(^{210}Pb_0(1 - z/(z + U_B)) + {}^{210}Pb\ z/(z + U_B))e^{(-z/U_B)}}{S} \quad (2)$$

The modification in Eq. (2) splits the filling of burrows into two parts: an exponentially decreasing (with depth) portion that fills burrows with surface particles, and another portion that fills with particles from the same depth to take into account lateral transport through burrow-wall collapse. Simulations using this modified regeneration model fit the $^{210}Pb_{ex}$ profiles observed at the two muddy marsh sites better than the previous model. However, if burrow-wall collapse is involved, there will not only be lateral filling of burrows with sediment from the same depth; sediment from above will also fall downward into the burrow; thus, advective transport and net movement of the bulk sediment at depth will occur. Accordingly, lateral filling, as described by Eq. (2), cannot be an accurate conceptual model for burrow-wall collapse.

To investigate how sediments are mixed by fiddler-crab burrowing, we expanded LABS to explicitly simulate the burrowing activities of fiddler crabs, accounting for the three different mixing modes mentioned above. Our model also simulates surface regeneration of excavated particles under different tidal conditions. With a selected mixing mode and a regeneration condition, the effects of burrowing parameters, such as burrowing frequency and burrow dimensions, can be studied with our model, including the resulting range and intensity of biogenic mixing. In this paper, we shall first present results of our numerical experiments on the effects of the different mixing modes, regeneration rates and values of burrowing parameters on predicted $^{210}Pb_{ex}$ profiles, and then, validate our model through simulations of actual $^{210}Pb_{ex}$ profiles. Finally, we investigate the exchange functions that could be used to describe fiddler-crab mixing in one-dimensional diagenetic equations.

2. Model and input parameters

The details of LABS are given elsewhere (Choi *et al.*, 2002), and not repeated here. Instead, this section describes the specific initial and input conditions of the model.

a. The sediment lattice

Our computer-generated sediment is a 2D (vertical) lattice, which is 30 cm wide and 32 cm deep, including a 4 cm water column, for all simulations except those with deep burrowing (25 cm mean burrow depth), where the matrix is 40 cm deep, including a 5 cm water column.

b. Sedimentation

We assume periodic sedimentation, i.e., four times per year, converted from a chosen annual sedimentation rate and constant bulk density. The value of the sedimentation rate for all simulations is set to 0.2 cm yr^{-1}, which is approximately the rate of sea level rise along the South Carolina coast during the last 50 years (McCraith *et al.*, 2003; Sharma *et al.*, 1987). To keep a constant water level over the sediment while particles are added randomly by sedimentation at the water-sediment interface, the same amount of particles is buried (removed) at the bottom of the model sediment. A mean constant porosity (0.9) over

the sediment slice is maintained during simulations; compacted areas and voids can and do develop, but on average the sediment has a porosity of 0.9.

c. The fiddler crabs and their burrows

For simplicity, we assume that fiddler crabs ideally only burrow vertically and will address nonvertical effects later in our discussion.

i. Burrow-and-fill modes. During burrow formation, we assume that two modes of particle transport may occur: (1) sediment particles can be removed uni-directionally to the sediment-water interface, which we regard as *excavation*, or (2) sediment particles can be pushed laterally aside and compacted into the burrow wall, which we term *partial compaction*. We also assume two modes of transport occur when burrows are later filled: (1) infilling by surface (interfacial) materials, and/or (2) collapse of the sidewall. Given these possibilities, we allow three possible burrow-and-fill modes in our simulations: (1) pure "removal-and-fill", i.e., pure excavation of burrows and infill with surface materials, (2) "removal-and-collapse", i.e., excavation of burrows and infilling with collapse of the burrow wall, and (3) "partial-compaction-and-collapse", i.e., a combination of excavation and compaction to form the burrow, with filling only by collapse of the burrow wall.

ii. Regeneration of the excavated particles. Given the variability in the frequency and extent of flooding in fiddler-crab habitats, we assume that excavated particles can be either (1) washed away and replaced by new particles (with input-source tracer activity/concentration) that are randomly distributed at the sediment-water interface, or (2) the excavated material can be randomly sedimented onto the interface without replacement by new material. The probability of a particle's replacement at the interface by new material is defined by an input *regeneration fraction* for a given simulation. There then exist two extreme cases: the surface sediment particles are either all new particles, with the highest tracer activities possible, when the regeneration fraction equals unity, or a homogeneous mixture of the particles excavated from different depths when the regeneration fraction is zero.

iii. Burrowing frequency. The term "burrowing frequency", $K_{B,}$ in the original regeneration model in Gardner *et al.* (1987) is ambiguous and, possibly, misleading. Instead of a real burrowing frequency i.e., the number of new burrows formed per unit surface area per unit time, i.e. $cm^{-2}\ yr^{-1}$, as used by McCraith *et al*. (2003), K_B is actually the total cross-sectional area of newly formed burrows (reworked area) per unit area of marsh surface per unit time, i.e. $cm^2\ cm^{-2}\ yr^{-1}$, as described by Gardner *et al*. (1987), which is equivalent to the product of the real burrowing frequency multiplied by the average (horizontal) cross-sectional area of a burrow. In this paper, we decompose K_B into two parameters: the real burrowing frequency (referred to as *Kb*) and the average diameter of a

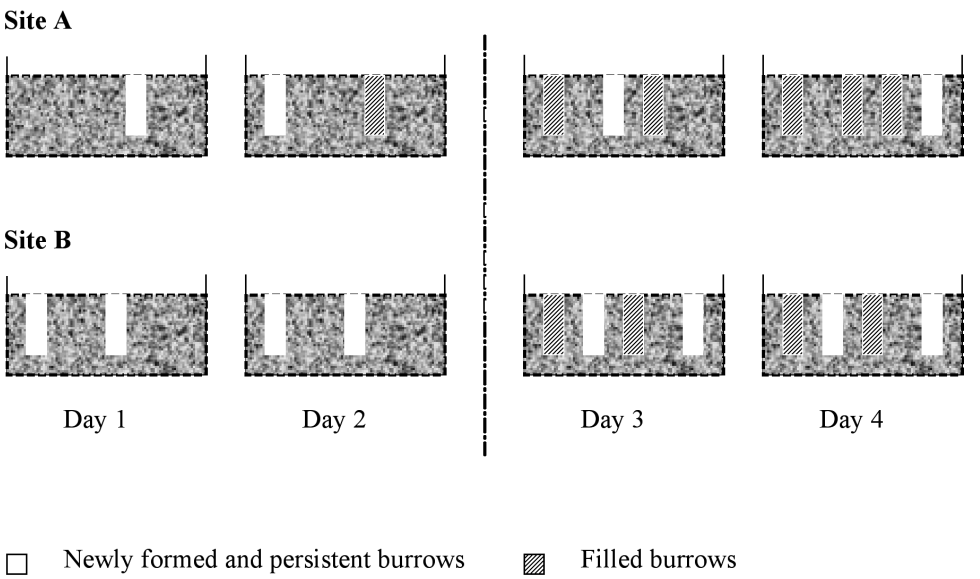

Figure 1. Demonstration of the effect of burrow density and new burrow formation rate on sediment reworking rate. The sediment reworking rate is the same at both hypothetical sites, even though the burrow density is greater at site B, i.e., on average one burrow forms every day.

burrow (referred to as *d*), as the circular cross-sectional area of a burrow can be calculated from the diameter of a burrow.

The new burrowing frequency, *Kb*, is one of the determinants of the sediment reworking rate, which is calculated by multiplying *Kb* by the volume of burrow formed. Since sediment reworking by fiddler crabs is only associated with burrowing events, i.e. the formation of new burrows and the filling and/or collapse of old burrows, the burrow density is not a reliable parameter to determine the sediment reworking rate. A higher burrow density does not necessarily indicate more burrows are formed during a certain period of time, if the burrows persist for a longer time. As demonstrated in Figure 1, the sediment reworking rate is the same at Site A and Site B over a given period of time, even though the burrow density at Site A is only half of that at Site B. At the sites studied by McCraith *et al*. (2003), the burrow density at the *Salicornia* site is less than half of the burrow density at the short-*Spartina* site, while the new burrow formation rate at the *Salicornia* site is almost four times that at the short-*Spartina* site!

In our simulations, we assume that burrow abundances are stable and that the rates of burrow appearance and disappearance are equal. To simplify the conversion from 3D field measurements to our 2D model parameters, we normalize the burrow density to one burrow within a *standard* square area of sediment surface. This means that only one burrow exists at a chosen time; this is possible because we have proven above that burrow (areal) density is not the determinant of mixing rate. To create the mixing effect of burrows

we then make this single burrow appear and disappear with a frequency needed to match the known burrowing rate. While counter intuitive, this is the correct way to proceed.

If we randomly take a vertical slice parallel to one side of a standard square, the probability that this slice cuts through a burrow equals the burrow diameter divided by the standard length. Therefore, the number of newly formed burrows in a 2D slice per unit-time is equivalent to (*Kb**standard-length*standard-length)*burrow-diameter/ standard-length, i.e. *Kb**standard-length*burrow-diameter. For our simulations, we chose 30 cm as the standard length. From the results of our preliminary simulation trials, the ratio between the survival time and re-colonization time does not produce significantly different results over a period of 100 years of simulation; thus, we simply convert the mean new burrow formation rate (*Kb*) of field measurements to the mean new burrow formation rate for the 2D model within a 30 cm width sediment and then to the mean survival time of burrows. For example, a mean 3D burrowing frequency of 0.256 cm^{-2} yr^{-1} with average burrow diameter of 2 cm is equivalent to 25 days of survival time. The probability distribution for the survival time of each burrow is assumed to be Gaussian, with a mean and a standard deviation approximated to field measurements. The burrow is placed randomly within the model. The distance between a new burrowing location and a previously abandoned burrow is also assumed to follow a Gaussian distribution, ranging between 4 and 14 cm.

iv. Locomotion speed. The locomotion rate of a fiddler crab moving down to dig a burrow is assumed to be 10 cm day^{-1} for each simulation.

v. Burrow depth (U_B). If, as the regeneration model assumes - see Eq. (1), the probability of a burrow reaching or exceeding depth z, $P(Z \geq z)$, is distributed exponentially, that is,

$$P(Z \geq z) = e^{-\beta z} \quad \text{where the } \beta = U_B^{-1} \tag{3}$$

then, the distribution function, $F(z)$, for the probability of the burrow's depth will be:

$$F(z) = P(Z < z) = 1 - P(Z \geq z) = 1 - e^{-\beta z} \tag{4}$$

and the probability density function is:

$$P(z) = F(z) = \beta e^{-\beta z}. \tag{5}$$

This latter result means that the probability of a burrow occurring at a given depth is exponential and, consequently, the probability is *extremely* biased to the small values of the distribution. In addition, for an exponential distribution, the mean $\mu = \beta^{-1} = U_B$ and the variance $\sigma^2 = \lambda^{-2} = U_B{}^2$; thus, μ is equal to σ. If one uses the "bias-corrected sample standard deviation", s_{N-1}, to estimate σ, the sample mean μ should be equal to, or almost equal to, s_{N-1}, which is not observed in field measurements of burrow depths (Bertness and Miller, 1984; Christy, 1982; Lim and Diong, 2003; McCraith *et al.*, 2003). Instead, we assume the probability of burrow depth follows approximately a Gaussian distribution,

rather than an exponential, with sample estimated mean and standard deviation derived from field measurements.

d. The sediment particles

i. Excess ^{210}Pb profiles. Initially, we set the activity on each particle to the value that would be expected at a given depth if only decay and sedimentation were operative (termed "control" conditions). In addition, without loss of generality, tracer activity is normalized to unit activity at the sediment-water interface. ^{210}Pb is continually supplied to the sediment-water interface, associated with the sediment particle fluxes during periodic sedimentation events and/or with the regeneration of excavated particles on the interface. Mean excess ^{210}Pb profiles are obtained by laterally averaging the current ^{210}Pb activities of every particle at each depth. The current ^{210}Pb activity on a particle is calculated from its initial/regeneration activity, the interval between the initial/regeneration time and the current time, and the decay constant of ^{210}Pb ($\lambda = 0.031076\ y^{-1}$).

ii. Particle movement profiles. Four types of particle movements are possible in fiddler-crab inhabited sediments: (1) biological removal of a particle from depth z to the sediment-water interface when a burrow is excavated, (2) displacement of a particle from a thin layer (1 cm) at the interface into the sediment at depth z when an abandoned burrow is filled-in with surface materials, (3) movement of a particle to a certain depth z_i within the sediment from all depths z_j above z_i when a burrow wall collapses, and 4) packing of particles into the borrow wall, which may result in some vertical (up or down) displacement of a particle. The frequency of each type of movement (particle^{-1} yr^{-1}) is calculated by dividing the number of movements by the simulation time period and the average number of particles at a selected depth, a number that can be regarded as constant because the porosity of the sediment is stable during a simulation. Following tradition (Boudreau and Imboden, 1987), the frequency of biological delivery from depth z_j to depth z_i per unit depth is referred as the "exchange function".

3. Simulation results

a. ^{210}Pb profiles

We shall first explore the effect of mixing modes, regeneration rate and burrowing parameters, i.e., burrowing frequency, burrow diameter and depth, on ^{210}Pb profiles through a series of simulations. We will also validate our model by comparing model predicted ^{210}Pb profiles, produced using observed values of burrowing parameters from three marsh sites as input parameters, with the actual excess ^{210}Pb profiles at these same sites. The control ^{210}Pb profile in each graph is produced under identical conditions without mixing.

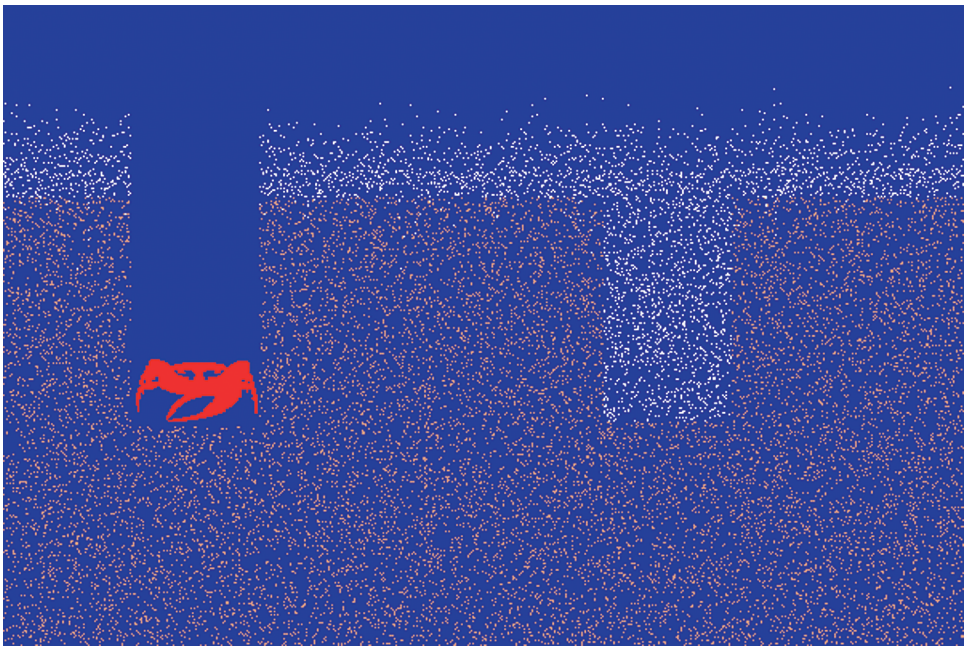

Figure 2. Visualization of a LABS simulation of fiddler-crab activity that produces removal-and-fill mixing, this time with complete regeneration of excavated particles. $d = 2.0$ cm; $Ub = 8$ cm; white marks initial surface and regenerated particles.

b. Removal-and-fill

Visualizations of fiddler-crab mixing in removal-and-fill mode are illustrated in Figures 2 and 3. For all visualizations, white pixels denote the "surface zone" and regenerated particles, which are associated with the highest activity of the tracer ^{210}Pb. As shown in these figures, the crab burrows down vertically and excavates all the particles from the burrow onto the sediment-water interface; then the abandoned burrow is filled with surface particles, while maintaining the same porosity as the sediment in its vicinity; therefore, the same number of sediment particles excavated out from the burrow subsequently fill it in. In the simulation with 100% regeneration of excavated particles (Fig. 2), the abandoned burrow is filled entirely with white particles, while the abandoned burrow is filled with a mixture of white and brown particles in the simulation without regeneration (Fig. 3). (Remember that regeneration means excavated particles are replaced by "new" particles with the highest allowed tracer activity.)

Figure 4 illustrates the influence of the regeneration fraction on the shape of ^{210}Pb profiles in simulations with removal-and-fill mixing. Each data point in this figure, as in all graphs that follow, is the mean of five model outcomes; standard errors, which are quite small compared with mean values for all simulations, are omitted to maintain clarity. Each profile in this figure is produced under exactly the same conditions and with the same

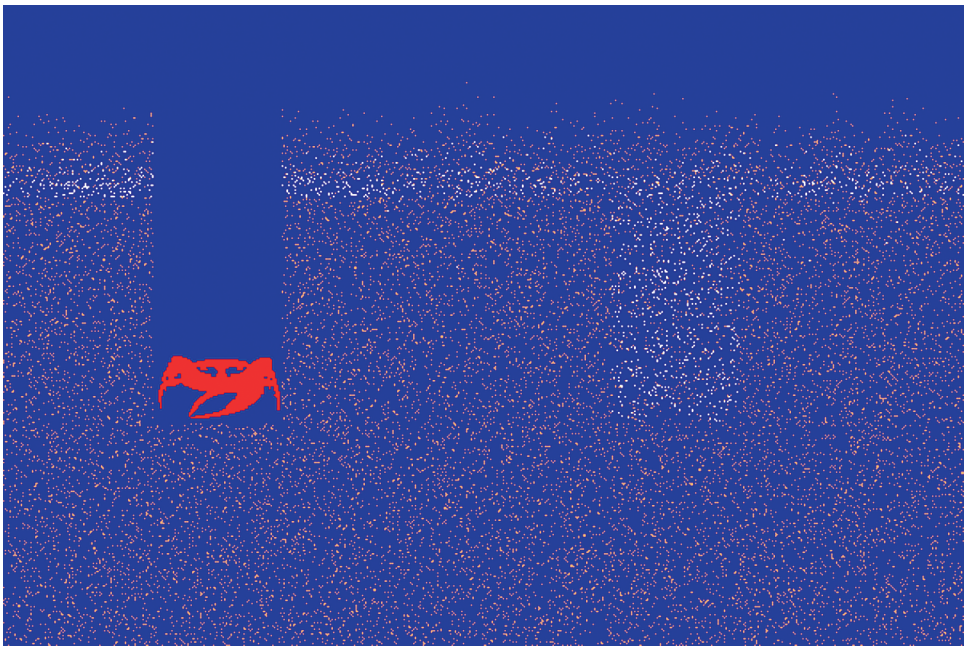

Figure 3. Visualization of a LABS simulation of fiddler-crab activity that produces removal-and-fill mixing, with no regeneration of excavated particles. $d = 2.0$ cm; $Ub = 8$ cm; and white marks initial surface particles.

burrowing parameters, including a burrowing frequency of 0.128 cm^{-2} yr^{-1}, a common *mean* burrow depth of 8 cm, and an identical burrow diameter of 2.0 cm. Variability in model output is due to random processes within LABS, e.g., choice of burrowing spot, burrow survival times, actual depth of burrowing, etc.

As can be seen in Figure 4, without regeneration ($r = 0$), the ^{210}Pb profile has a nearly vertical upper portion within the intensively mixed zone. Near the sediment-water interface, there are indications of a "boundary layer" with a sharp gradient in activity. The lower portion or tail under the mixed layer decays exponentially, similar to the control profile. This profile is consistent with the shape predicted by Boudreau and Imboden (1987) in their theory of nonlocal mixing (refer to their Fig. 2). With increasing regeneration ($r > 0$), the upper (mixed) portion of the ^{210}Pb profiles becomes progressively more enriched with high-activity regenerated surface material. A small near-surface portion (the boundary layer) contains even more high-activity material and therefore, a sharp interface gradient develops, as the regeneration rate increases. The apparent surficial boundary layer is partially an artifact and partially a real phenomenon. Straight horizontal sampling of an uneven sediment-water interface, in part, creates this change in the gradient by mixing materials at different relative depths. Nevertheless, the anchoring of the surface

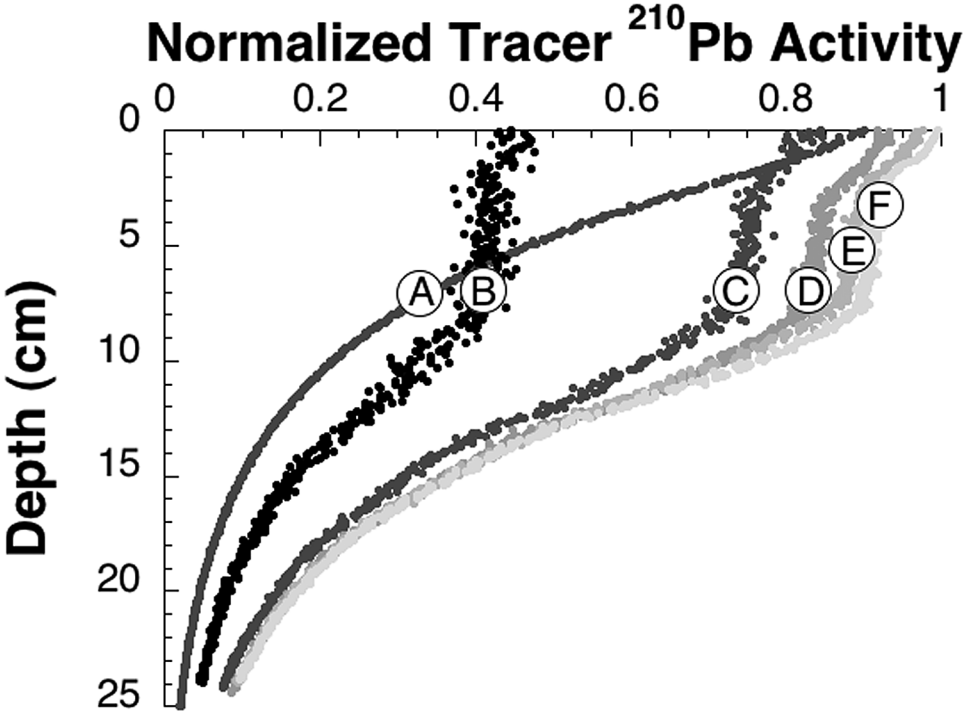

Figure 4. ^{210}Pb depth profiles created with different regeneration fractions (r) of particles excavated to the surface during removal-and-fill mixing. A: control (simulation without fiddler-crab mixing); B: $r = 0$; C: $r = 0.25$; D: $r = 0.5$; E: $r = 0.75$; F: $r = 1$ (100% regeneration). Simulation time = 100 years; Sedimentation rate = 0.2 cm yr^{-1}; Kb = 0.128 cm^{-2} yr^{-1}; d = 2.0 cm; Ub = 8 cm.

activity caused by regeneration also contributes to the boundary layer, as seen in Boudreau and Imboden (1987), and that effect is real.

Figure 5 displays the effects of varying the burrowing frequency on the shape of ^{210}Pb profiles, without regeneration (Fig. 5a) and with 100% regeneration (Fig. 5b). In the case without regeneration, as the intensity of the burrowing frequency decreases, ^{210}Pb profiles progressively approach the control profile. These profiles again resemble the steady-state tracer profiles theoretically predicted for burrow-and-fill mixing with surficial infilling (refer to Fig. 7 in Boudreau and Imboden, 1987). With total regeneration of excavated particles (Fig. 5b), the upper portions of the ^{210}Pb profiles slide toward the control curve and gradually become less vertical while the boundary layer stretches and disappears with decreasing burrow density. Note that the profiles with no regeneration of surface material ($r = 0$) conserve the total inventory (standing stock) of tracer. The profiles with regeneration ($r > 0$) do not, because regeneration creates a source of new tracer and a sink for subsurface particles with lower tracer activities.

Another factor that influences the reworking of sediments is the burrow diameter, d,

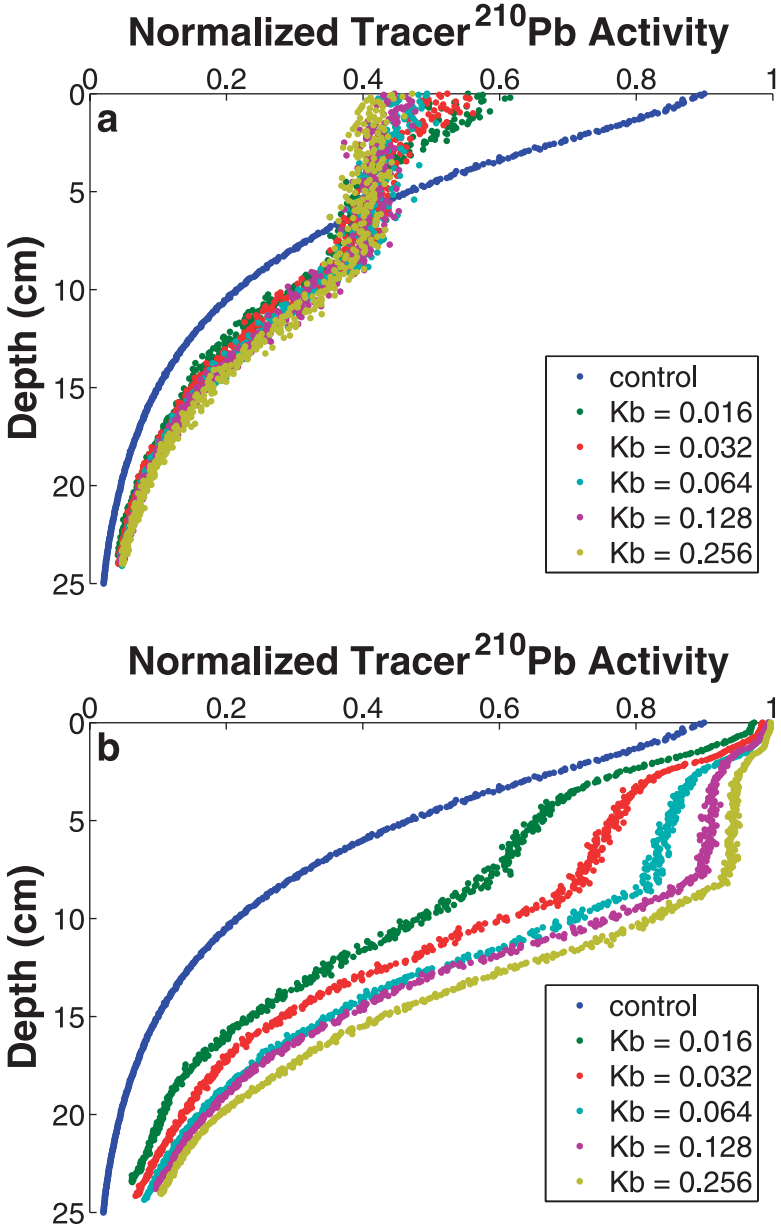

Figure 5. ^{210}Pb depth profiles that result from different burrowing frequencies (*Kb*, cm^{-2} yr^{-1}) with removal-and-fill mixing: (a) profiles without regeneration ($r = 0$); (b) profiles with complete regeneration ($r = 1$). Control is a simulation without fiddler-crab mixing. Simulation time = 100 years; Sedimentation rate = 0.2 cm yr^{-1}; $d = 2.0$ cm; $Ub = 8$ cm.

which results in changes to the ^{210}Pb profiles like those produced by varying the burrowing frequency - see Figure 6. Comparing Figures 5 and 6, we can see that varying the burrow diameter causes substantially greater changes in ^{210}Pb profiles than varying the burrowing frequency. For example, for a twofold change in the diameter from 2 cm to 1 cm, with the same *Kb* of 0.128 cm^{-2} yr^{-1}, the separation between the upper potions of the resulting ^{210}Pb profiles (Fig. 6) is approximately the same as the separation produced by a fourfold change of burrowing frequencies, from 0.128 to 0.032 cm^{-2} yr^{-1} in Figure 5, with a constant burrow diameter of 2 cm. This phenomenon is easily understood because the fraction of a standard cross-section that is reworked is calculated by multiplying the burrowing frequency by the square of the burrow diameter.

Finally, the influence of varying burrow depth on the shapes of ^{210}Pb profiles is illustrated in Figure 7. Without regeneration of excavated particles (Fig. 7b), the ^{210}Pb profile predicted by the simulation with greater mean burrow depth has a longer and more vertical upper portion, as we would expect. Note the conservation of inventory in this case. With complete regeneration of excavated particles (Fig. 7a), greater mean burrow depths create more vertical and longer upper portions to the predicted ^{210}Pb$_{ex}$ profiles, as well as sharper interface gradients. In contrast to the profiles generated without regeneration, these vertical upper portions stay at almost the same activity when the burrow depth changes; this is again related to the source role of regeneration.

c. Removal-and-collapse

Figure 8 illustrates a simulation of fiddler-crab mixing in removal-and-collapse mode, with all excavated sediment particles regenerated ($r = 1$). As in Figures 2 and 3, the crab digs a vertical burrow with all particles excavated from the burrow onto the sediment-water interface; however, the abandoned burrow is now filled with particles from the collapse of the burrow wall. As can be seen in Figure 8, the filled burrow area is nearly conical, instead of rectangular.

For comparison, we ran simulations for this mixing mode with the same regeneration rates, burrowing frequencies, burrow diameters and depths as those used in simulations with burrow-and-fill mixing. Figure 9 shows the results with varying regeneration rates (r). Predicted ^{210}Pb$_{ex}$ profiles in Figure 9 resemble those in Figure 4, except that the upper portion of each profile decreases smoothly (almost linearly) with depth, without the near-surface boundary layer. In fact, all simulations with varying burrowing frequency and burrow diameter and depth in this mode produce ^{210}Pb profiles that differ in only minor ways from profiles generated with removal-and-fill; for concision, only one example with changing burrow diameter is presented for comparison in Figure 10. Collapse of the wall creates an advection that stretches the boundary layer so that it is no longer evident. Note that the profiles produced from simulations without regeneration resemble the steady-state tracer profiles predicted theoretically by simultaneous constant nonlocal exchange and conveyor-belt removal (refer to Fig. 4 in Boudreau and Imboden, 1987).

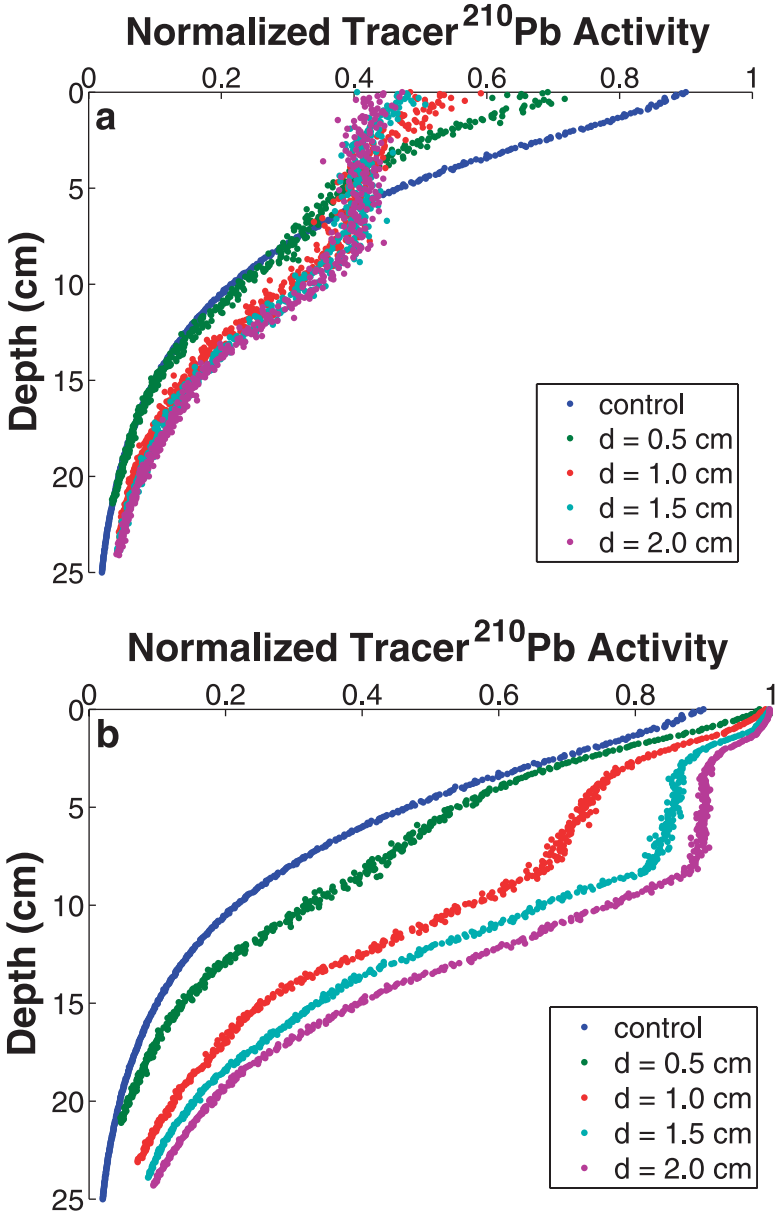

Figure 6. ^{210}Pb depth profiles that result from different burrow diameters (d, cm) with removal-and-fill mixing: (a) with complete regeneration ($r = 1$); (b) without regeneration ($r = 0$). Control is a simulation without fiddler-crab mixing. Simulation time = 100 years; Sedimentation rate = 0.2 cm yr^{-1}; $Kb = 0.128$ cm^{-2} yr^{-1}; $Ub = 8$ cm.

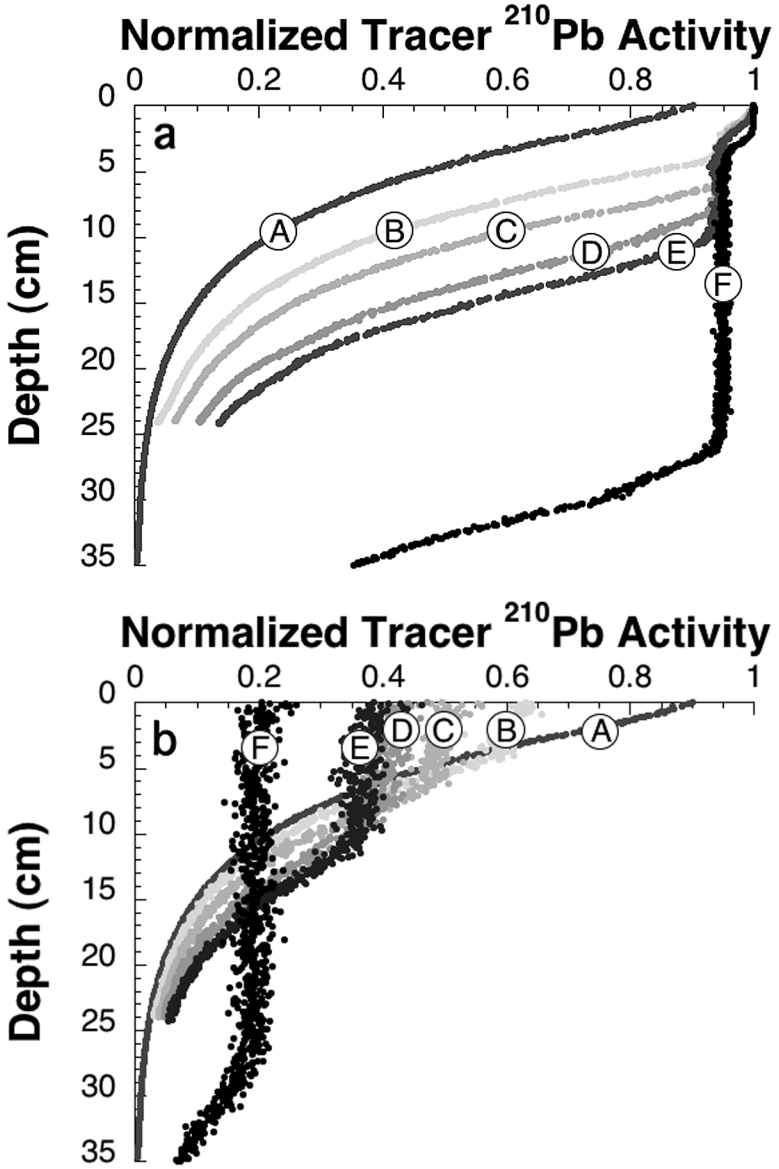

Figure 7. ^{210}Pb depth profiles created with a range of burrow depths (*Ub*) with removal-and-fill mixing: (a) without regeneration ($r = 0$); (b) with complete regeneration ($r = 1$). Labels indicate - A: control (simulation without fiddler-crab mixing); B: $Ub = 4$ cm; C: $Ub = 6$ cm; D: $Ub = 8$ cm; E: $Ub = 10$ cm; F: $Ub = 25$ cm. Simulation time = 100 years; Sedimentation rate = 0.2 cm yr^{-1}; $Kb = 0.256$ cm^{-2} yr^{-1}; $d = 2.0$ cm.

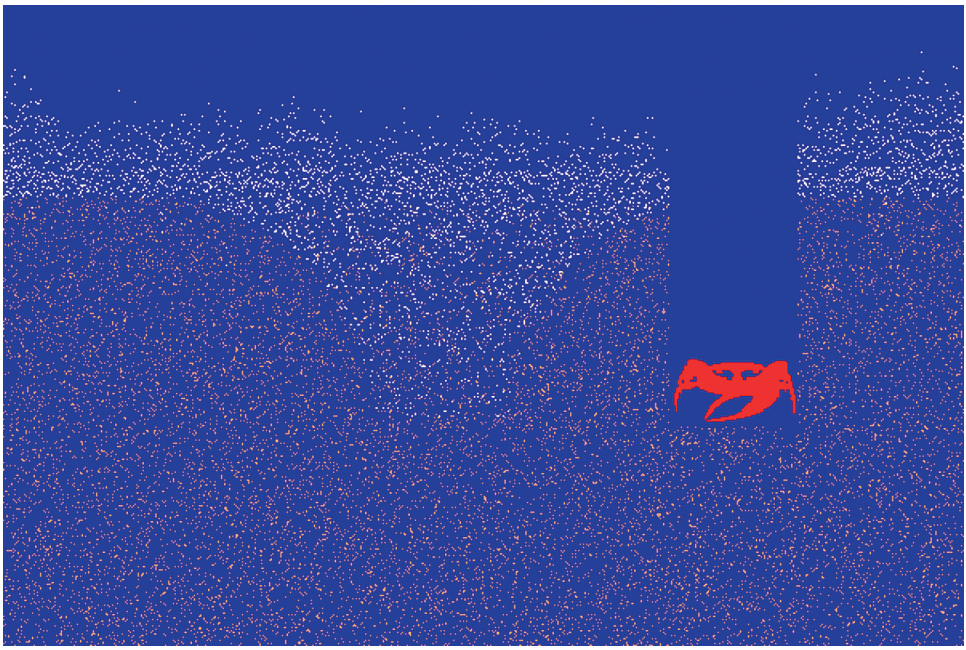

Figure 8. Visualization of a LABS simulation of fiddler-crab activity that leads to removal-and-collapse mixing, with complete regeneration of excavated particles ($r = 1$). $d = 2.0$ cm; $Ub = 8$ cm; white particles are either initially at the surface or are regenerated.

d. Partial-compaction-and-collapse

A visualization of fiddler-crab mixing with partial-compaction-and-collapse is presented in Figure 11. The excavated sediment particles on the sediment surface are all regenerated. As showed in this figure, the crab pushes aside some sediment particles while excavating the burrow, specifically half the particles within the burrow in this case, and compacts them into the burrow wall; therefore, a structure of denser burrow wall material is created, instead of removing all the particles from burrow to the sediment-water interface. Filling of the abandoned burrow occurs by collapse, as in the previous example. The filled burrow again appears conical, but the white regenerated particles are more concentrated in the upper portion and the lower portion is almost completely filled with older brown particles.

Figure 12 illustrates the effect of lining the burrow with excavated material on fiddler-crab mixing, without regeneration (Fig. 12a) and with complete regeneration (Fig. 12b). For these simulations, a constant burrow diameter (2.0 cm) was used, as well as the same mean burrow depth and mean burrowing frequency as in the simulations presented in Figure 10. The parameter e denotes the excavation fraction parameter, which is the probability of a particle being excavated, i.e., removed from depth onto the sediment interface. With the partial-compaction-and-collapse mode, a particle is either excavated or pushed aside and compacted into the burrow wall; therefore, if $e = 0.5$, for example, a

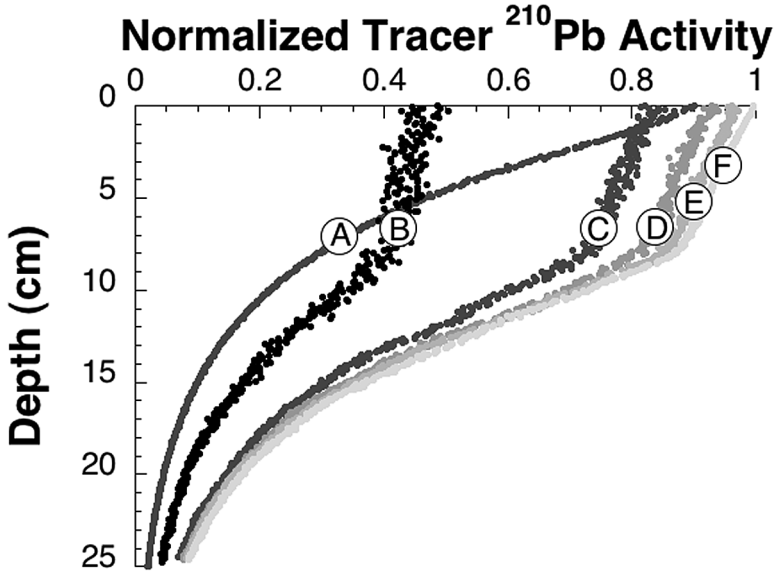

Figure 9. ^{210}Pb depth profiles create by different regeneration fractions (r) of excavated particles during removal-and-collapse mixing. Labels - A: control (simulation without fiddler-crab mixing); B: $r = 0$; C: $r = 0.25$; D: $r = 0.5$; E: $r = 0.75$; F: $r = 1$. Simulation time = 100 years; Sedimentation rate = 0.2 cm yr^{-1}; $Kb = 0.128$ cm^{-2} yr^{-1}; $d = 2.0$ cm; $Ub = 8$ cm.

particle has a 50% chance of being excavated to the surface and a 50% chance of being pushed aside. As can be seen in Figure 12, with decreasing e, i.e., increasing compaction, the predicted $^{210}Pb_{ex}$ profile becomes less vertical in the mixed zone. The resulting $^{210}Pb_{ex}$ profiles with varying e are, however, less "steep" than those created by changing the burrow diameter, d, in the removal-and-collapse mode (Fig. 9).

e. Trial predictions

We used observations of burrowing frequency, as well as burrow diameter and depth, from two low-marsh sites ("creek bank" and "short-*Spartina*") and one high-marsh site ("*Salicornia*") from McCraith *et al*. (2003) as input parameters for trial simulations to validate our model. For each trial, only the regeneration fraction and the mixing mode were varied to create our predictions. The regeneration fraction mainly affects the initial value of surface material and not the shape of the profile, given a chosen mixing mode; it was adjusted only to bring predicted and observed surface values into accord. The choice of mixing mode offers some flexibility, particularly with respect to the degree of compaction, e.

For the two low-marsh sites, as shown in Figure 13, the best concurrence between predictions (dark grey) and data (circles) are obtained by using complete regeneration and *partial-compaction-and-collapse* ($e = 0.6$ for creek bank; $e = 0.5$ for short-*Spartina*).

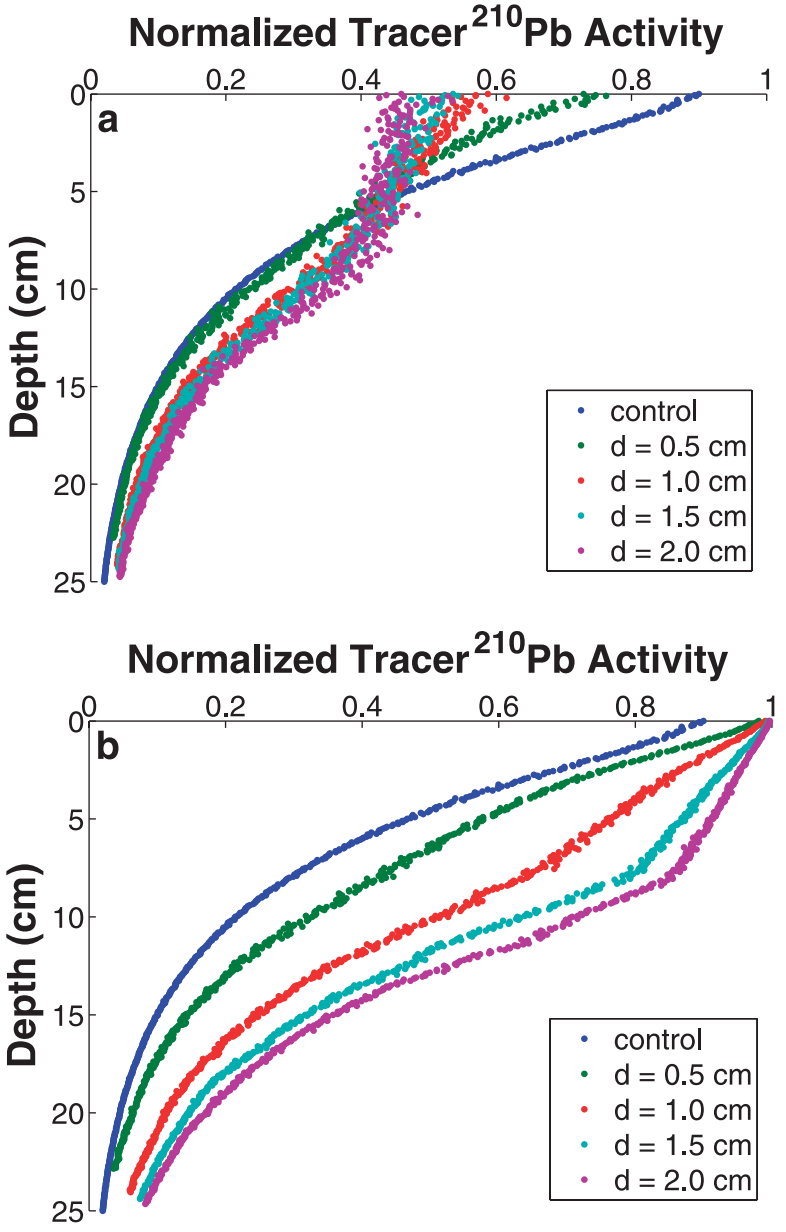

Figure 10. ^{210}Pb depth profiles created with different burrow diameters (d) with removal-and-collapse mixing: (a) without regeneration ($r = 0$) and indicated diameters; (b) with complete regeneration ($r = 1$) and various diameters. Control is a simulation without fiddler-crab mixing. Simulation time = 100 years; Sedimentation rate = 0.2 cm yr^{-1}; Kb = 0.128 cm^{-2} yr^{-1}; Ub = 8 cm.

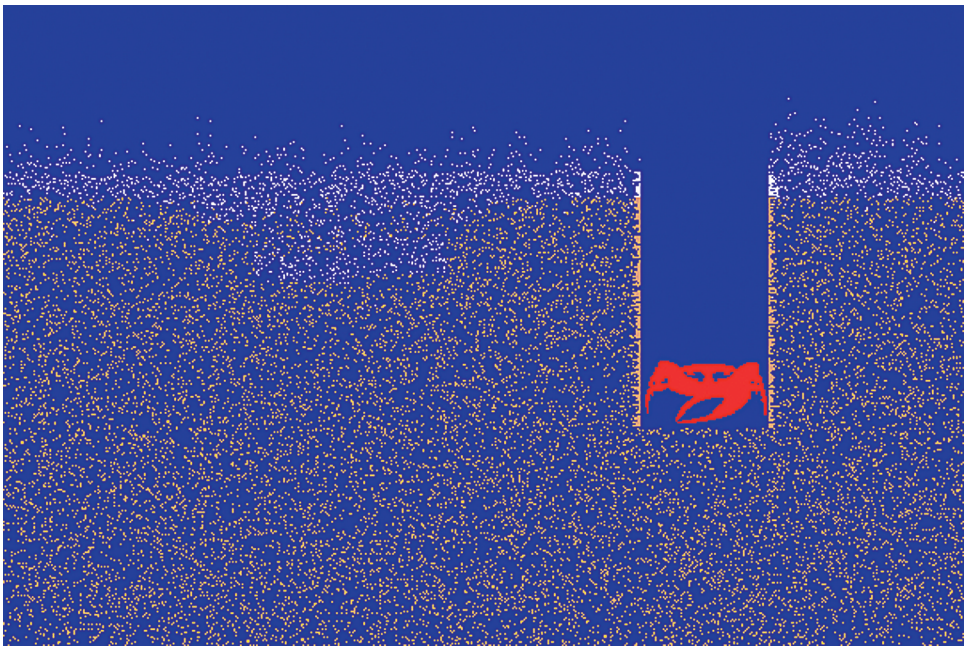

Figure 11. Visualization of a LABS simulation of fiddler-crab activity that leads to partial-compaction-and-collapse mixing, with complete regeneration of excavated particles. $d = 2.0$ cm; $Ub = 8$ cm; white particles are either initially at the surface or are regenerated.

Complete regeneration is supported by the tidal conditions observed at low-marsh sites, which are regularly flooded by the tide. Our *predicted* ^{210}Pb profiles (Fig.13a and Fig. 13d) are in remarkably good agreement with the field data within the mixed layer, providing better concurrence than the fits using the original and modified regeneration models (McCraith *et al.*, 2003). Below the mixed layer, our predicted profiles have lower activities than the field measurements for reasons that we shall discuss further below. Compared with these best predictions, simulations with removal-and-fill (Fig. 13b and Fig. 13e) and removal-and-collapse (Fig. 13c and Fig. 13f) modes produce $^{210}Pb_{ex}$ profiles that are more vertical in shape, and thus, higher than the data at the low-marsh sites. The root mean square (RMS) of the prediction errors at each sampled depth is plotted in Figure 14 to compare prediction fit-goodness for these three modes. The RMS was calculated as:

$$RMS(n_d) = \sqrt{\frac{1}{n_d}\sum_{i=1}^{n_d} e_i^2} \tag{6}$$

where n_d is the number of depths at which both field data and our prediction model results were sampled, and e_i is the prediction error, which is the difference between the data value

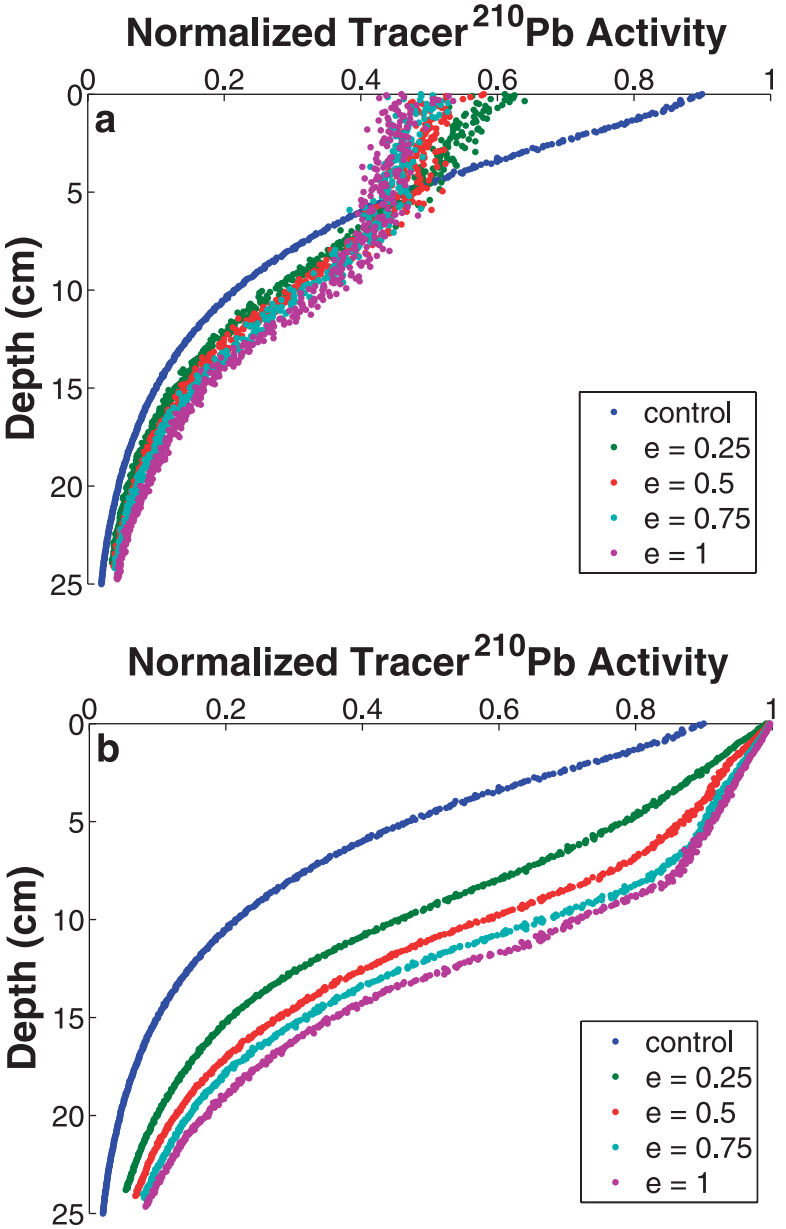

Figure 12. ^{210}Pb depth profiles generated with different excavation fraction (e) with partial-compaction-and-collapse mixing: (a) without regeneration and indicated excavation fractions; (b) with complete regeneration. Control is a simulation without fiddler-crab mixing. Simulation time = 100 years; Sedimentation rate = 0.2 cm yr^{-1}; Kb = 0.128 cm^{-2} yr^{-1}; Ub = 8 cm.

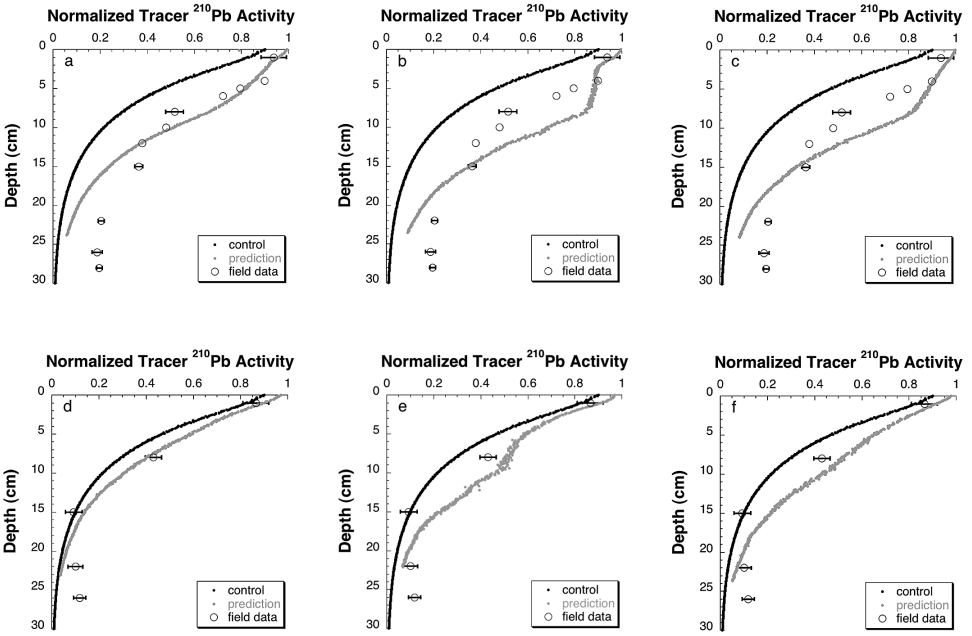

Figure 13. Trial predictions of ^{210}Pb depth distributions at two low-marsh sites. Diagrams a-c: creek bank (Kb = 0.2 cm^{-2} yr^{-1}; d = 1.4 cm; Ub = 8 cm) with partial compaction-and-collapse, removal-and-fill, and removal-and-collapse mixing, respectively. Diagrams d-f: short *Spartina* (Kb = 0.01 cm^{-2} yr^{-1}; d = 1.9 cm; Ub = 10 cm) with partial compaction-and-collapse, removal-and-fill, and removal-and-collapse mixing, respectively. Observed excess ^{210}Pb data from McCraith *et al.* (2003).

and the prediction value at a sampled depth. The model with partial compaction produces remarkably lower errors that are also small in absolute terms.

Best predictions for the *Salicornia* site (Fig. 15) are obtained with *pure-removal-and-fill* and 50% regeneration (r = 0.5). The predictions with *removal-and-collapse* and *partial-compaction-and-collapse* are less vertical in shape (not shown) and thus not as consistent with the data. The predicted $^{210}Pb_{ex}$ profile with d = 1.3 cm (Fig. 15a) and field data both contain a near-surface mixed layer up to 8 cm; however the model-generated profile has lower activity than the observations in this situation. Considering that the burrows of *U. pugilator* are either J- or L-shaped and the ratio of burrow length to burrow depth is 12:8 at the *Salicornia* site, a larger burrow diameter is expected in cross-section at depth z; therefore, in this case, the diameter was adjusted to 2.0 cm and a better prediction is obtained (Fig. 15b). The RMS (n_d) values are compared in Figure 16 for these two predictions.

f. Removal and infill frequencies

Profiles of removal frequencies for simulations with removal-and-fill mixing are almost identical to the profiles of infilling frequencies - see Figure 17. Note that these are

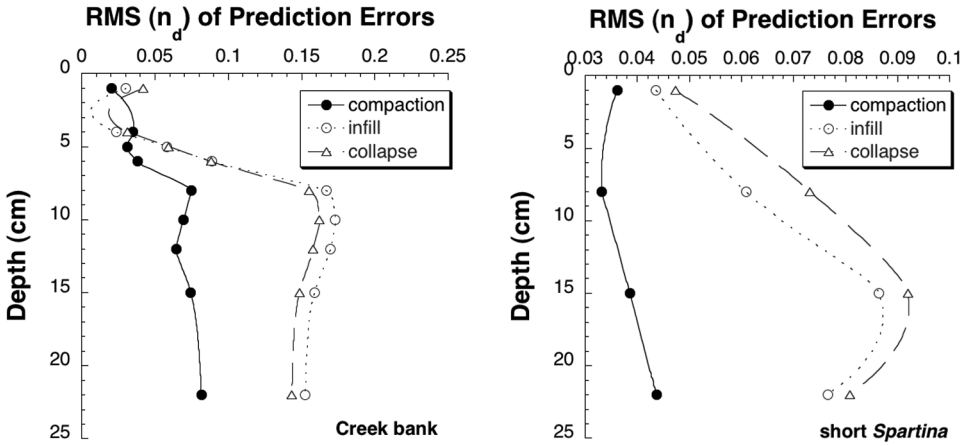

Figure 14. The RMS (n_d) of the prediction errors for the Creek Bank and short-Spartina sites for each of the three mixing modes.

calculated quantities, not inputs. The frequencies are almost constant up to the mean burrow depth and then they vanish with depth as excavation vanishes. This shape corresponds to the integral of the Gaussian distribution of burrow depths. As the burrowing frequency increases, the resulting removal/infilling frequency increases accordingly, thus explaining the development of a "well-mixed" surface layer. Simulations with removal-and-collapse produce identical removal frequency profiles as those with removal-and-fill (results not presented); however, infilling frequency in the former case (Fig. 18) decreases exponentially with depth.

g. Exchange functions

The exchange function accounts for the fraction of sediment particles transferred per unit length and time to a given depth z from (and to) all other depths. Exchange functions constitute fundamental descriptions of sediment mixing, and they can be placed in 1D conservation (diagenetic) equations to account for mixing, without recourse to highly simplified, a priori models that often lack justification, e.g. biodiffusion. Such functions are displayed as 3D plots in this section. The z-coordinate specifies the depth to which the particles are transferred, while the z'-coordinate specifies the originating depth of the particles. The E-coordinate (vertical) provides the magnitude of the exchange function.

First, let us look at the 3D plots of the exchange function obtained from simulations with a set of burrowing parameters (Kb = 0.256 cm^{-2} yr^{-1}; U_B = 8.0 cm; d = 2.0 cm) with burrow-and-collapse mixing. As can be seen in Figure 19a, the plot has two ridges, one near the z-axis and another, weaker one, along the diagonal of the z and z' plane, i.e., $z = z$'. (Note: A trend that is symmetric around the line $z = z$' indicates particle movement that tends to be local and symmetric, and therefore, diffusive.) In downward mixing, particles are only transferred from layers above a given z and so, as shown in the graph, the "fraction

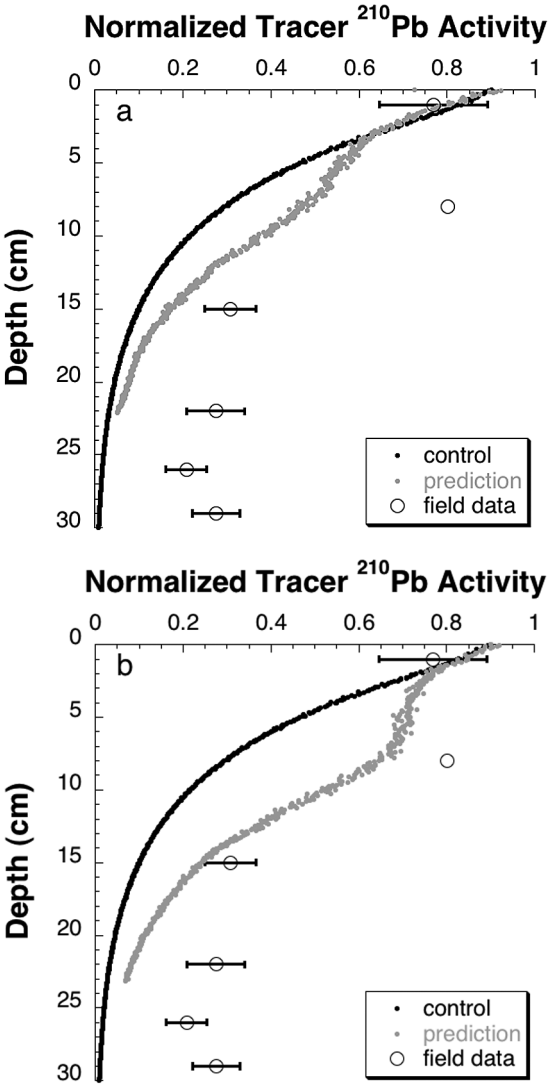

Figure 15. Trial prediction of the ^{210}Pb depth distribution at the high-marsh site, *Salicornia*: (a) for a burrow diameter of 1.3 cm; (b) for a burrow diameter of 2.0 cm. Additionally $Kb = 0.04$ cm^{-2} yr^{-1}; $UB = 8$ cm. 1. $d = 1.3$ cm, and 2. $d = 2.0$ cm. Observed excess ^{210}Pb data from McCraith *et al.* (2003).

transferred" peaks near the origin ($z = 0$, $z' = 0$) and decreases with depth, while the mixing distance spectrum (in the z' direction) gets broader with depth z. By taking a slice in the z-z' plane near $z' = 0$, we get an exponential decrease, which resembles the plot of infilling frequency - Figure 17b. If we take slices elsewhere along the z'-coordinate, we

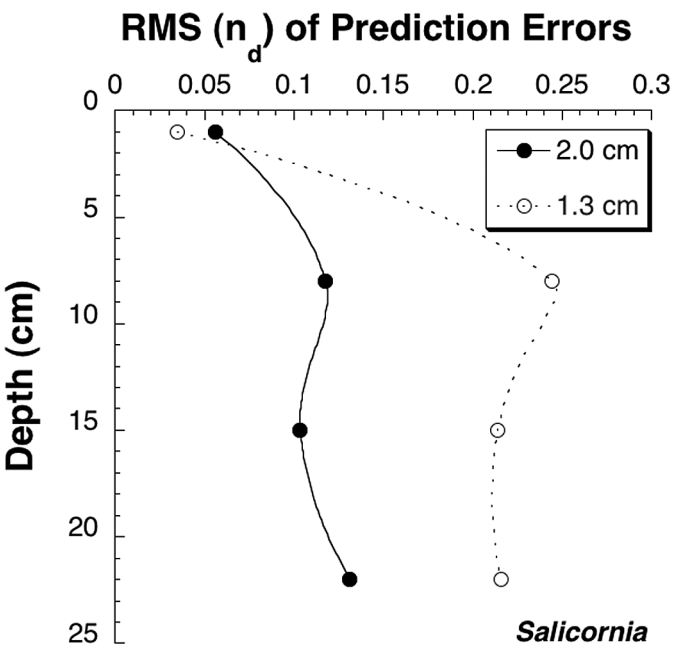

Figure 16. The RMS (n_d) of the prediction errors for the high-marsh site.

will also obtain a series of exponentially decreasing curves, which start gradually from deeper points and with lower values and become flatter and shorter.

The effect of varying the burrowing frequency on the exchange function can be appreciated by comparing Figure 19a through 19d. With decreasing burrowing frequency, the transfers between depths became less frequent, but the range of mixing depth and the mixing length spectrum do not change.

Simulations with different mean burrow depths are showed in Figures 20a to 20d. With deeper burrows, the mixed layer also deepens and, as a consequence, the maximum mixing length spectrum becomes wider; at the same time, the intensity of mixing increases with deeper burrowing.

Finally, we display the dramatic transformation of the exchange function when mixing is due to partial-compaction-and-collapse (Fig. 21). Starting with Figure 21a, the exchange function is plotted for the same simulation conditions as in Figure 19b with burrow-and-collapse mixing ($e = 1.0$, i.e. no compaction for burrowing) and the same set of burrowing parameters. The plots in Figures 21b to 21d display the effects of decreasing the excavation fraction, i.e. an increasing probability of compaction. The exchange function transforms systematically from an exponential nonlocal form to a semi-local form by narrowing the mixing length spectrum and limiting the mixing transfers to a narrow range of depths. The mixing in Figure 21d is not diffusion, as the distribution is a asymmetric about $z = z'$. Compaction of particles into the burrow wall can result in a diffusion-like spread of

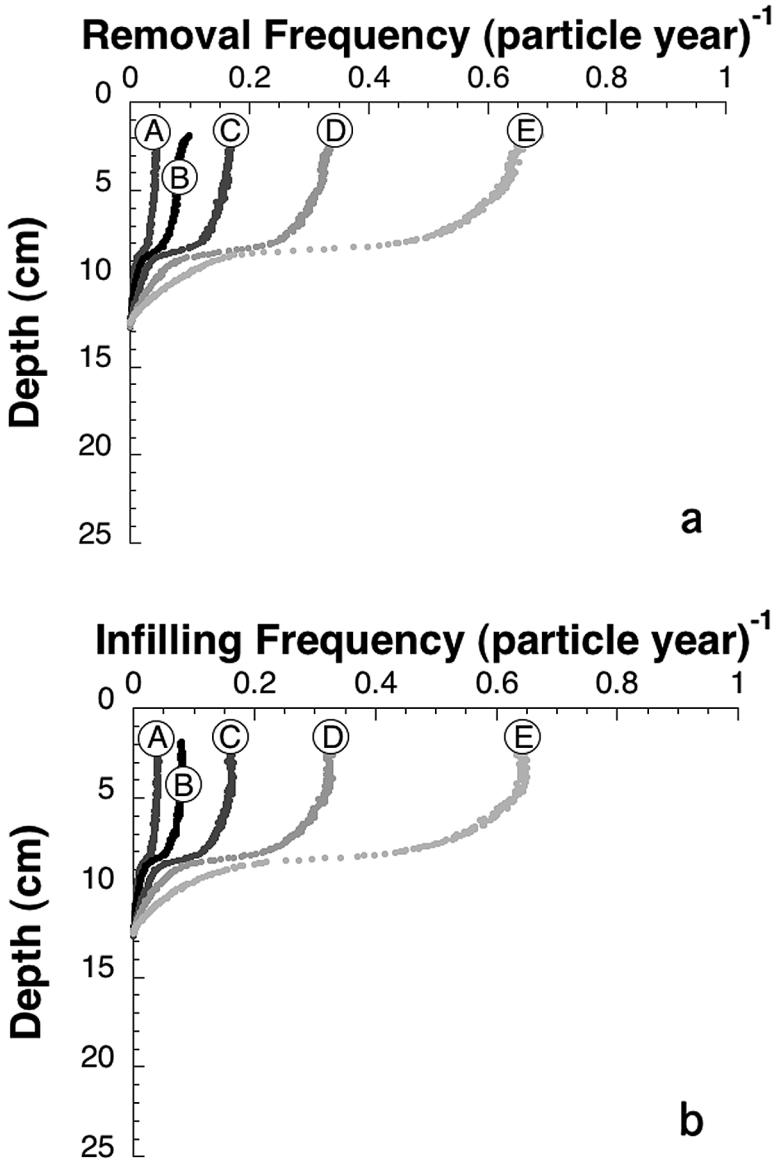

Figure 17. Removal and infilling frequencies for different burrowing frequencies (*Kb*) with removal-and-fill mixing: (a) the frequency of particle removal from depth to the water sediment interface when burrows are excavated; (b) the frequency of infilling by particles from sediment surface (1 cm thin layer) to depth when abandoned burrows were filled. Labels - A: $Kb = 0{,}016$; B: $Kb = 0.032$; C: $Kb = 0.064$; D: $Kb = 0.128$; E: $Kb = 0.256$ cm^{-2} yr^{-1}. Sedimentation rate $= 0.2$ cm yr^{-1}; $d = 2.0$ cm; $Ub = 8$ cm.

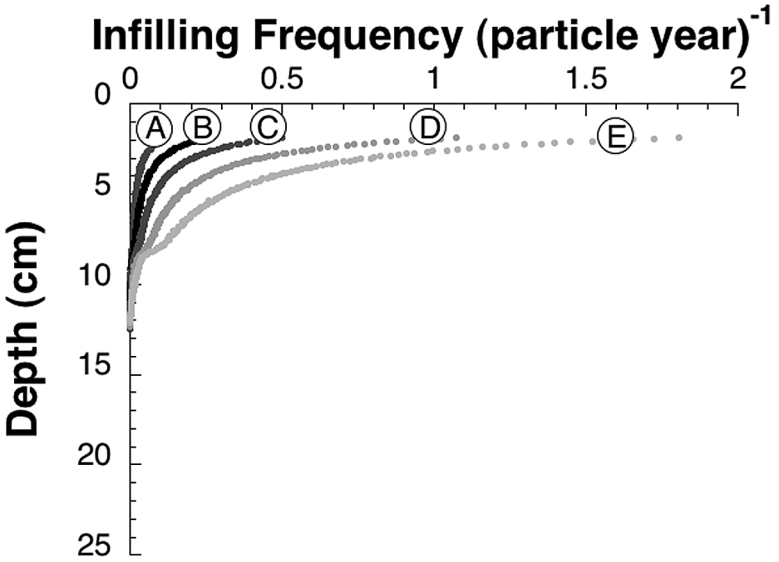

Figure 18. Infilling frequency for different burrowing frequencies (*Kb*) with removal-and-collapse mixing. Labels - A: $Kb = 0.016$; B: $Kb = 0.032$; C: $Kb = 0.064$; D: $Kb = 0.128$; E: $Kb = 0.256$ cm^{-2} yr^{-1}. Sedimentation rate = 0.2 cm/yr; $d = 2.0$ cm; $Ub = 8$ cm.

particles as they can move both upward and downward during this process, but the collapse of the burrows causes a net downward motion and generates the asymmetry in the exchange function.

4. Discussion and conclusions

LABS aims at creating a synthetic ecology that sufficiently mimics reality to allow investigation of the relationships between biological causes and observed effects, such as the distribution of tracers with depth in the sediment. We previously found that LABS provided valuable information about tracer mixing created by small deposit feeders (Boudreau *et al.*, 2001; Reed *et al.*, 2006). With the current contribution, we extend this positive judgment to a new class of organisms, fiddler crabs, which are thought to create mixing of a highly directional character.

The mechanisms behind fiddler-crab mixing are varied, and we identify three such variants: (1) burrow-and-fill mixing, where burrows are filled exclusively with slumped surface materials, (2) removal-and-collapse, where filling is caused by collapse of the burrow walls, and (3) partial-compaction-and-collapse, where burrowing is accomplished in part by excavation to the surface and partially by compacting sediment into the burrow walls and adjacent sediment, with subsequent filling by collapse.

It is not clear when or why each of these three modes would dominate in nature, but we have found that best predictions to observed data from Bly Creek (NC) are produced by

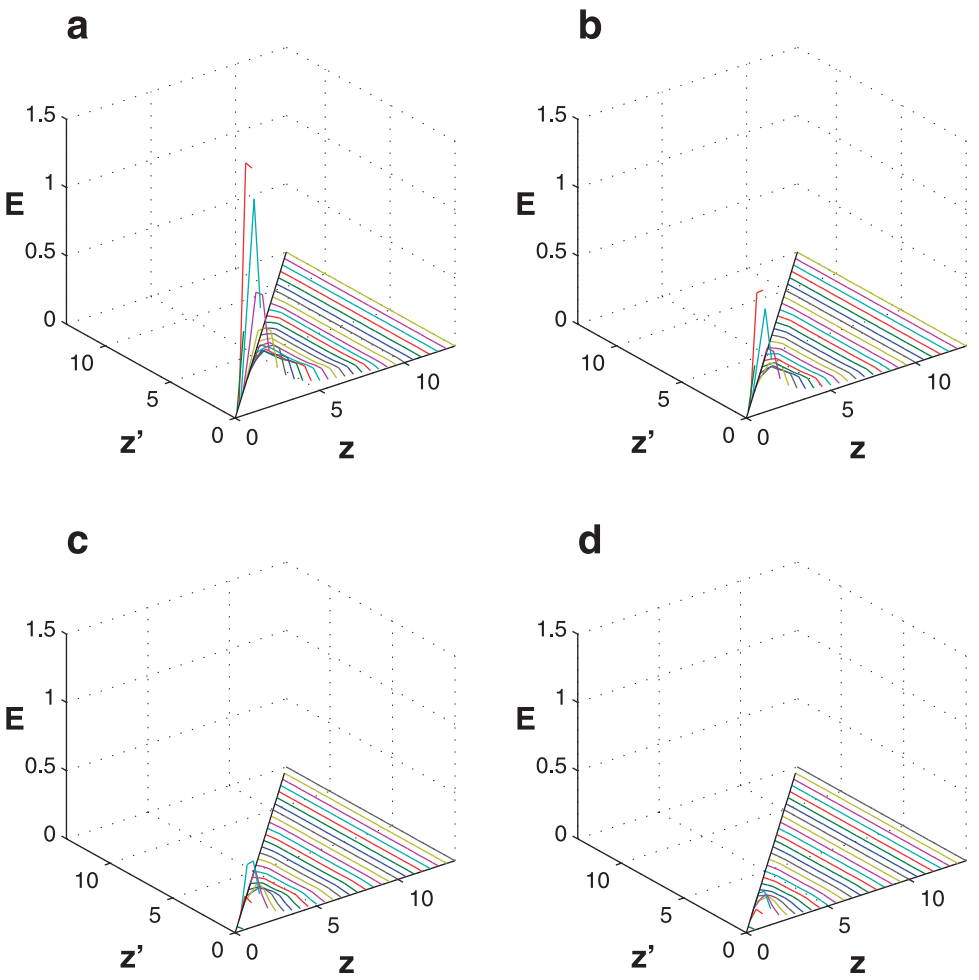

Figure 19. Exchange functions, E, between depth z and any other depth z' for different burrowing frequencies (Kb) with removal-and-collapse mixing. (a) $Kb = 0.256$ cm^{-2} yr^{-1}; (b) $Kb = 0.128$ cm^{-2} yr^{-1}; (c) $Kb = 0.064$ cm^{-2} yr^{-1}; (d) $Kb = 0.032$ cm^{-2} yr^{-1}. Sedimentation rate = 0.2 cm yr^{-1}; $d = 2.0$ cm; $Ub = 8$ cm.

assuming that two different modes operate at different sites. At the two low-marsh sites ("creek bank" and "short-*Spartina*"), excess ^{210}Pb profiles are best predicted assuming *partial-compaction-and-collapse* (Fig. 13). This result suggests that to construct a burrow, a mud fiddler crab may pack significant amounts of sediment into the burrow wall, rather than excavate all of the sediment to the interface. Abandoned burrows are then filled by burrow-wall collapse. We can find no direct observational evidence regarding burrow construction by mud fiddler crabs; however, there is one important field observation that may support our partial-compaction-and-collapse hypothesis indirectly. Comparison of the

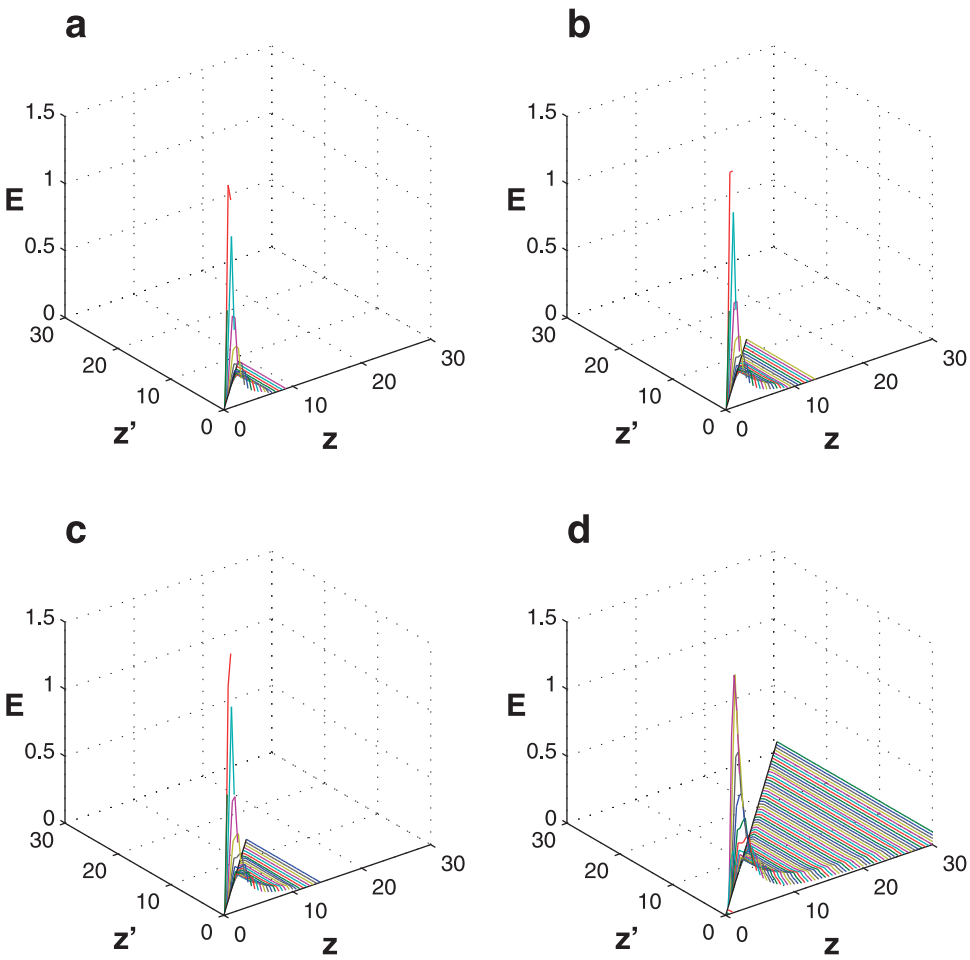

Figure 20. Exchange functions, E, between depth z and any other depth z' for different burrow depths (Ub) with removal-and-collapse mixing. (a) Ub = 6 cm; (b) Ub = 8 cm; (c) Ub = 10 cm; (d) Ub = 25 cm. Sedimentation rate = 0.2 cm yr^{-1}; Kb = 0.256 cm^{-2} yr^{-1}; d = 2.0 cm.

sediment reworking rate measured by burrow casts versus burrow pellets indicate that, while these two measurements match well for 2 replicates in May and June for a sand-fiddler-inhabited site, the burrow pellets estimate is 26% of the burrow-cast value at the mud fiddler-crab-inhabited site in May.

Dorgan *et al.* (2005) have advanced a mechanism for burrow formation without excavation. These investigators propose that some organisms burrow by propagating a crack in the direction of motion. While that original study focused on the motion of worms, Dorgan *et al.* (2006) have extended their ideas to include other infauna, such as clams. Mud fiddler crabs *may* utilize the same mechanism, which might explain the predominance of

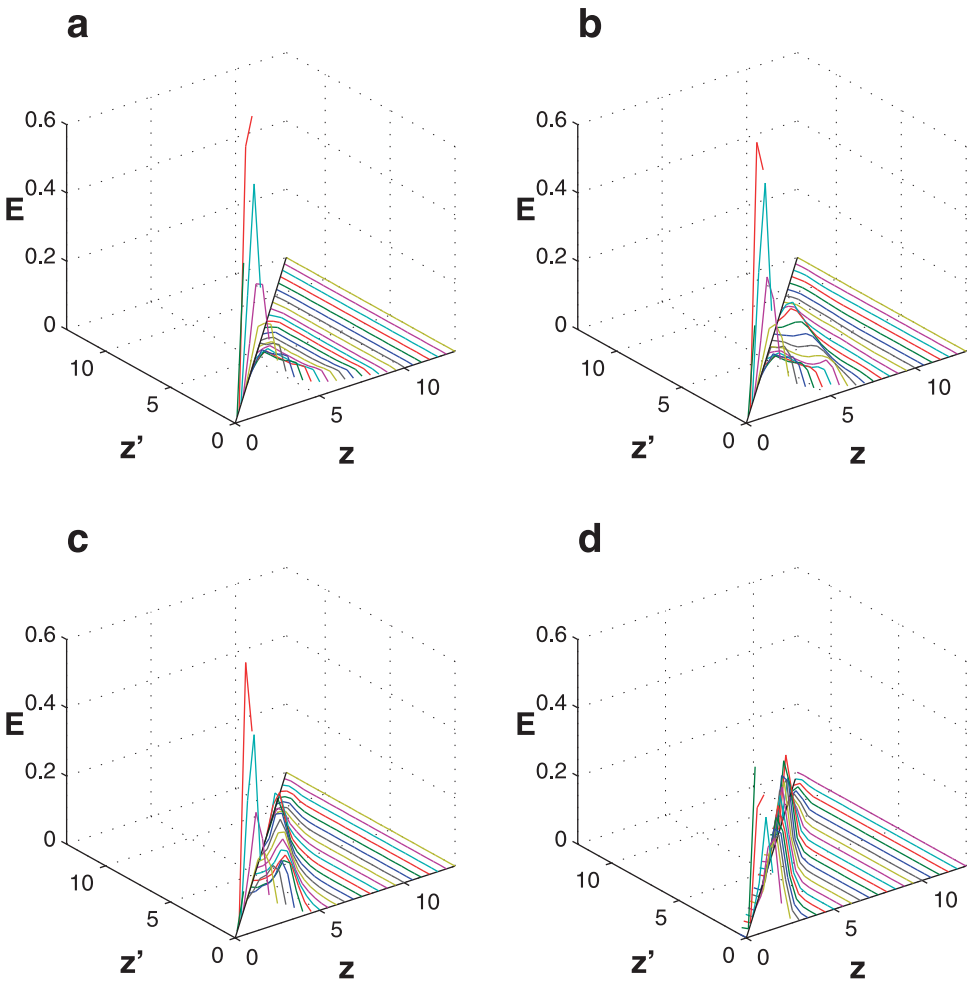

Figure 21. Exchange functions, E, between depth z and any other depth z' for different excavation fractions (e) with partial-compaction-and-collapse mixing. (a) $e = 1$; (b) $e = 0.75$; (c) $e = 0.5$; (d) $e = 0.25$. Sedimentation rate $= 0.2$ cm yr^{-1}; $Kb = 0.128$ cm^{-2} yr^{-1}; $d = 2.0$ cm, $Ub = 8$ cm.

compaction in burrowing, but we are not advocating this explanation, simply noting the possibility. By contrast, crack propagation is not an effective means of burrowing in sands.

Excess ^{210}Pb in the mixed surface zone at the high-marsh site is near vertical and our predictions with *removal-and-fill* best match the data, which is consistent with the fact that high-marsh sites are only flooded by the highest spring tides (McCraith *et al.*, 2003). The high-marsh site is sandy, with low porosity and inhabited by sand fiddler crabs (McCraith *et al.*, 2003).

In comparing the two types of sites, we see that the degree of regeneration of excavated sediment particles is another major factor in the distribution of excess ^{210}Pb. Simulations

with a greater regeneration fraction of excavated particles produce ^{210}Pb profiles with higher average activity in the mixed layer. This result agrees with the original regeneration model (Gardiner *et al.*, 1987). The actual regeneration fraction in the field is probably determined by two factors: (1) how often a site is flushed by tides, and (2) whether the invading materials are constituted of fresh sediment or "old" sediments flushed from another site (Gardner and Sharma, 1987). Our best predictions for the two low-marsh sites occur with complete regeneration of excavated particles.

Below the mixed layer, the field measurements of excess ^{210}Pb activities are all higher than those we predict. The field profiles do not asymptote exponentially to zero, as expected for an advection-decay system; instead, the profiles attain a constant nonzero value with depth. Normally, a quasi-exponentially decrease of excess ^{210}Pb to zero at around 10 to 15 cm below the surface mixed layer is expected and often found in such sediments, and excess ^{210}Pb activities at depths of 20 to 25 cm are observed only when long burrows (70 to 115 cm) exist (e.g., Benninger *et al.*, 1979). Therefore, we assume that the difference between simulated and field excess ^{210}Pb profiles in the lower portion may come from: (1) mixing in deeper layers by other crustaceans, such as mud crabs; and (2) other factors that might affect accurate measurement of excess ^{210}Pb activities, such as compaction, post-depositional nuclide migration, smearing by coring, mixing and slumping due to gas bubbling, possible artifacts of the activity of the crabs in the laboratory after collection, diffusion of Rn generated by the decay of Ra and so on, as mentioned by McCraith *et al.* (2003).

More generally, our simulations have shown that for removal-and-fill mixing, the removal frequency resembles the infill frequency at depth and both of these suggest a Gaussian distribution of burrow depths. This means that the rate of removal of particles from depth z is equal to the rate of infilling of particles to that depth and the rate of removal/infilling is constant at depth within the mixed layer if all burrows reach the same depth. The removal/infilling rate at depth is correlated with burrowing frequency. The mean burrow depth determines the depth of the removal-and-fill mixing, while the distribution of burrow depths will influence the shape of the removal/infilling frequency profiles.

On the other hand, removal-and-collapse differs mechanistically from removal-and-fill in two respects: (1) the infilling frequency of surface particles decreases quasi-exponentially with depth to near zero approximately at the mean burrow depth, and (2) the infilling particles moving to depth z are not restricted to surface particles, but also come from sediment layers above z, as shown by the exchange functions, which are of exponential form. This result illustrates that, when burrow-wall collapse is involved, the mechanism of removal-and-fill mixing by fiddler crabs resembles "conveyor-belt" mixing. This result also suggests that wall collapse mixing as formulated in the modified version of the regeneration model (Eq. 2) is not entirely correct. Note also that with increasing compaction, the exchange function transforms from an exponential form to a quasi-local form (Fig. 21), which indicates that local mixing becomes appreciable with compaction.

This explains why the actual excess ^{210}Pb profiles were not as vertical as predicted by the regeneration model, even with high burrowing frequency, as in the "creek bank" site.

Finally, actual excess ^{210}Pb profiles are usually obtained by taking finite-thickness lateral slices of sediment, typically 1 cm thick; thus, the resulting resolution may not be precise enough to tell the differences between $^{210}Pb_{ex}$ profiles caused by infilling versus collapse near the sediment-water interface. In addition, infilling of surface materials and wall collapse may actually happen simultaneously. However, a nearly vertical excess ^{210}Pb profile appears to indicate that high intensity burrow-and-fill mixing has occurred at a sample site, if the site is dominated by fiddler crabs. This conclusion is also reached in other studies (Boudreau and Imboden, 1987; Gardner *et al.*, 1987).

The above analysis of mixing by fiddler crabs was possible because of the power of LABS. The synthetic data produced allows us to investigate this phenomenon without the costs associated with field investigations. LABS is not a replacement for experimental and observational studies, but a supplement when faced with the realities of the time and money needed to acquire such data. LABS also allows manipulation of its "environment", which is difficult in nature.

Acknowledgments. We wish to thank the US Office of Naval Research, and Program Manager, Dr. Jim Eckman, for generous support for this project (N00014-02-1-0107).

REFERENCES

Benninger L. K., R. C. Aller, J. K. Cochran and K. K. Turekian. 1979. Effects of biological sediment mixing on the SUP-210 Pb chronology and trace metal distribution in a Long Island Sound sediment core. Earth Planet. Sci. Lett., *43*, 241-259.

Bertness M. D. and T. Miller. 1984. The distribution and dynamics of *Uca Pugnax* (Smith) burrows in a New England salt marsh. J. Exper. Mar. Biol. Ecol., *83*, 211-237.

Boudreau B. P., J. Choi, F. Meysman and F. Francois-Carcaillet. 2001. Diffusion in a lattice-automaton model of bioturbation by small deposit feeders. J. Mar. Res., *59,* 749-768.

Boudreau B. P. and D. M. Imboden. 1987. Mathematics of tracer mixing in sediments; III, The theory of nonlocal mixing within sediments. Am. J. Sci., *287*, 693-719.

Choi J., F. Francois-Carcaillet and B. P. Boudreau. 2002. Lattice-automaton bioturbation simulator (LABS); implementation for small deposit feeders. Comp. Geosci., *28*, 213-222.

Christy J. H. 1982. Burrow structure and use in the sand fiddler crab, *Uca pugilator* (Bosc). Animal Behaviour, *30*, 687-694.

Dorgan K. M., P. A. Jumars, B. D. Johnson and B. P. Boudreau. 2006. Macrofaunal burrowing: The medium is the message. Oceanogr. Mar. Biol.: An Ann. Rev., *44*, 85-121.

Dorgan K. M., P. A. Jumars, B. Johnson, B. P. Boudreau and E. Landis. 2005. Burrow extension by crack propagation. Nature, *433*, 475.

Gardner L. R., P. Sharma and W. S. Moore. 1987. A regeneration model for the effect of bioturbation by fiddler crabs on (super 210) Pb profiles in salt marsh sediments. J. Environ. Radioactivity, *5*, 25-36.

Gribsholt B., J. E. Kostka and E. Kristensen. 2003. Impact of fiddler crabs and plant roots on sediment biogeochemistry in a Georgia saltmarsh. Mar. Ecol. Progr. Ser., *259*, 237-251.

Katz L. C. 1980. Effects of burrowing by the fiddler crab, *Uca pugnax* (Smith). Estuar. Coastal Mar. Sci., *11*, 233-237.

Koretsky, C. M., C. Meile and P. Van Cappellen. 2002. Quantifying bioirrigation using ecological parameters: a stochastic approach. Geochem. Trans., *3*, 17-30.

Kristensen E. and D. M. Alongi. 2006. Control by fiddler crabs (*Uca vocans*) and plant roots (*Avicennia marina*) on carbon, iron, and sulfur biogeochemistry in mangrove sediment. Limnol. Oceanogr., *51,* 1557-1571.

Lim S., S. L. and C. H. Diong. 2003. Burrow-morphological characters of the fiddler crab, *Uca Annulipes* (h. Milne Edwards, 1837) and ecological correlates in a Lagoonal Beach on Pulau Hantu, Singapore. Crustaceana, *76*, 1055-1069.

McCraith B. J., L. R. Gardner, D. S. Wethey and W. S. Moore. 2003. The effect of fiddler crab burrowing on sediment mixing and radionuclide profiles along a topographic gradient in a southeastern salt marsh. J.Mar. Res., *61*, 359-390.

Montague C. L. 1981. The influence of some larger animals on subsurface metabolic processes in intertidal sediments. Estuaries, *4*, 289.

—— 1980. A natural history of temperate western Atlantic fiddler crabs (genus *Uca*) with reference to their impact on the salt marsh. Contributions to Marine Science., University of Texas, *23,* 25-55.

Nielsen O. I., E. Kristensen, and D. J. Macintosh. 2003. Impact of fiddler crabs (*Uca* spp.) on rates and pathways of benthic mineralization in deposited mangrove shrimp pond waste. J. Exper. Mar. Biol. Ecol., *289*, 59-81.

Reed D. C., K. Huang, B. P. Boudreau and F. J. R. Meysman. 2006. Steady-state tracer dynamics in a lattice-automaton model of bioturbation. Geochimica et Cosmochimica Acta, *70,* 5855-5867

Sharma P., L. R. Gardner, W. S. Moore and M. S. Bollinger. 1987. Sedimentation and bioturbation in a salt marsh as revealed by ^{210}Pb, ^{137}Cs, and ^{7}Be studies Limnol. Oceanogr., *32*, 313-326.

Received: *16 January, 2007*; revised: *17 July, 2007*.